Paper

Exact pairwise error probability analysis of space-time codes in spatially correlated fading channels

Tharaka A. Lamahewa, Marvin K. Simon, Thushara D. Abhayapala, and Rodney A. Kennedy

Abstract—In this paper, we derive an analytical expression for the exact pairwise error probability (PEP) of a space-time coded system operating over a spatially correlated slow fading channel using a moment-generating function-based approach. This analytical PEP expression is more realistic than previously published exact-PEP expressions as it fully accounts for antenna spacing, antenna geometries (uniform linear array, uniform grid array, uniform circular array, etc.) and scattering models (uniform, Gaussian, Laplacian, Von-Mises, etc.). Inclusion of spatial information provides valuable insights into the physical factors determining the performance of a space-time code. We demonstrate the strength of our new analytical PEP expression by evaluating the performance of two space-time trellis codes proposed in the literature for different spatial scenarios.

Keywords— Gaussian Q-function, modal correlation, moment-generating function, MIMO system, non-isotropic scattering, space-time coding.

1. Introduction

Space-time coding combines channel coding with multiple transmit and multiple receive antennas to achieve bandwidth and power efficient high data rate transmission over fading channels. The performance criteria for space-time codes have been derived in [1] based on the Chernoff bound applied to the pairwise error probability (PEP). In general, the Chernoff bound is quite loose for low signal-to-noise ratios. In [2], the exact-PEP of space-time codes operating over independent and identically distributed (i.i.d.) fast fading channels was derived using the method of residues. A simple method for exactly evaluating the PEP based on the moment generating function associated with a quadratic form of a complex Gaussian random variable [3] is given in [4] for both i.i.d. slow and fast fading channels. The fading correlation effects on the performance of space-time codes were investigated in [5]. There, the exact-PEP results derived in [2] were further extended to spatially correlated slow fading channels with the use of residue methods. In [5], the correlation is calculated in terms of the correlation between channel gains, but there is no direct realizable physical interpretation to the spatial correlation. Therefore, existing PEP expressions derived in the literature do not provide insights into the physical factors determining the performance of a space-time code operating over correlated fading channels. In particular, the effect of antenna spacing, spatial geometry of the antenna arrays and the non-isotropic scattering environments on the performance of space-time codes are of interest.

In this paper, using the MGF-based approach presented in [4], we derive an analytical expression for the exact-PEP of a space-time coded system operating over a spatially correlated slow fading channel. This expression is more realistic than previously published exact-PEP expressions, as it fully accounts for antenna placement along with non-isotropic scattering environments. In this work, we use a recently developed novel spatial channel model [6, 7] to incorporate the above factors in to the exact-PEP expression of a space-time coded system. Using this analytical exact-PEP expression, one can evaluate the performance of a space-time code applied to a MIMO system in any general spatial scenario (*antenna geometries*: uniform linear array (ULA), uniform grid array (UGA), uniform circular array (UCA), etc., *scattering models*: uniform, Gaussian, Laplacian, Von-Mises, etc.) without the need for extensive simulations. We provide an analytical technique which can be used to evaluate the exact-PEP in closed form. The strength of our new analytical exact-PEP expression is demonstrated by evaluating the performance of a 4-state QPSK space-time trellis code with two transmit antennas proposed by Tarokh *et al.* [1] and a 16-state QPSK space-time trellis code with three transmit antennas proposed by Zuho-Chen *et al.* [8] for different spatial scenarios.

The rest of this paper is organized as follows. Section 2 reviews the spatial channel model derived in [6]. Section 3 formulates the exact-PEP of a space-time coded system operating over a spatially correlated channel and Section 4 discusses a technique which can be used to obtain analytical solutions for the exact-PEP. Section 5 is devoted to examples, where we investigate the effects of antenna spacing, antenna configuration and scattering channel correlation for two space-time trellis codes. Finally, conclusions are drawn in Section 6.

Notations. Throughout the paper, the following notations will be used: $[\cdot]^T$, $[\cdot]^*$ and $[\cdot]^\dagger$ denote the transpose, complex conjugate and conjugate transpose operations, respectively. The symbols $\delta(\cdot)$ and $\otimes$ denote the Dirac delta function and matrix Kronecker product, respectively. The notation $E\{\cdot\}$ denotes the mathematical expectation, $\mathrm{Q}(y) = \frac{1}{\sqrt{2\pi}} \int_y^\infty e^{-x^2/2} dx$ denotes the Gaussian Q-function, $\mathrm{vec}(A)$ denotes the vectorization operator which stacks the columns of A, and $\lceil . \rceil$ denotes the ceiling operator. The matrix I_n is the $n \times n$ identity matrix.

2. System model

Consider a multi input multi output (MIMO) system consisting of n_T transmit antennas and n_R receive antennas. Let $x_n = [x_1^{(n)}, x_2^{(n)}, \cdots x_{n_T}^{(n)}]^T$ denote the space-time coded signal vector transmitted from n_T transmit antennas in the nth symbol interval and $X = [x_1, x_2, \cdots, x_L]$ denote the space-time code representing the entire transmitted signal, where L is the code length. Assuming quasi-static fading, the signals received at n_R receiver antennas during L symbol periods can be expressed in matrix form as

$$Y = \sqrt{E_s}HX + N,$$

where E_s is the transmitted power per symbol at each transmit antenna and H is the $n_R \times n_T$ zero-mean complex valued channel gain matrix, N is the noise represented by an $n_R \times L$ complex matrix in which entries are zero-mean independent Gaussian distributed random variables with variance $N_0/2$ per dimension.

Spatial channel model. Using a recently developed spatial channel model [6], we are able to incorporate the antenna spacing, antenna placement and scattering distribution parameters such as mean angle-of-arrival (AOA), mean angle-of-departure (AOD) and angular spread, into the exact-PEP calculations of space-time coded systems. In this spatial channel model, MIMO channel is separated in to three physical regions of interest: scatterer free region around the transmitter antenna array, scatterer free region around the receiver antenna array and the complex random scattering media which is the complement of the unions of two antenna array regions. In other words, MIMO channel is decomposed into deterministic and random matrices, where the deterministic portion depends on the physical configuration of the transmitter and the receiver antenna arrays and the random portion represents the complex scattering media between the transmitter and the receiver antenna regions.

Let u_p, $p = 1, 2, \cdots, n_T$ be the position of pth transmit antenna relative to the transmitter antenna array origin and v_q, $q = 1, 2, \cdots, n_R$ be the position of qth receive antenna relative to the receiver antenna array origin. Assume that the scatterers are distributed in the farfield from the transmitter and the receiver antenna arrays and the two regions are distinct. Then the MIMO channel H has the decomposition

$$H = J_R H_S J_T^{\dagger}, \tag{1}$$

where J_R is the $n_R \times (2m_R + 1)$ receiver antenna array configuration matrix,

$$J_R = \begin{pmatrix} \mathscr{J}_{-m_R}(v_1) & \cdots & \mathscr{J}_{m_R}(v_1) \\ \mathscr{J}_{-m_R}(v_2) & \cdots & \mathscr{J}_{m_R}(v_2) \\ \vdots & \ddots & \vdots \\ \mathscr{J}_{-m_R}(v_{n_R}) & \cdots & \mathscr{J}_{m_R}(v_{n_R}) \end{pmatrix},$$

J_T is the $n_T \times (2m_T + 1)$ transmitter antenna array configuration matrix,

$$J_T = \begin{pmatrix} \mathscr{J}_{-m_T}(u_1) & \cdots & \mathscr{J}_{m_T}(u_1) \\ \mathscr{J}_{-m_T}(u_2) & \cdots & \mathscr{J}_{m_T}(u_2) \\ \vdots & \ddots & \vdots \\ \mathscr{J}_{-m_T}(u_{n_T}) & \cdots & \mathscr{J}_{m_T}(u_{n_T}) \end{pmatrix},$$

with $\mathscr{J}_n(x)$ defined as the spatial-to-mode function (SMF) which maps the antenna location to the nth mode of the region. The form which the SMF takes is related to the shape of the scatterer-free antenna region. For a circular region in 2-dimensional space, the SMF is given by a Bessel function of the first kind [6] and for a spherical region in 3-dimensional space, the SMF is given by a spherical Bessel function [7]. For a prism-shaped region, the SMF is given by a prolate spheroidal function [9]. Here, we consider only the 2-dimensional[1] scattering environment where antennas are encompassed in scatterer-free circular apertures. In this case, SMF is given by

$$\mathscr{J}_n(w) = J_n(k\|w\|)\mathrm{e}^{in(\phi_w - \pi/2)},$$

where $J_n(\cdot)$ is the Bessel function of integer order n, vector $w = (\|w\|, \phi_w)$ in polar coordinates is the antenna location relative to the origin of the aperture which encloses the antennas, $k = 2\pi/\lambda$ is the wave number with λ being the wave length and $i = \sqrt{-1}$. $M_T = (2m_T + 1)$ and $M_R = (2m_R + 1)$ are the number of effective communication modes[2] available in the transmitter and receiver regions, respectively. Note that, m_T and m_R are determined by the size of the antenna aperture, but not from the number of antennas encompassed in an antenna array. The number of effective communication modes (M) available in a region is given by [10]

$$M = 2\lceil \pi e r/\lambda \rceil + 1, \tag{2}$$

where r is the minimum radius of the antenna array aperture and $\mathrm{e} \approx 2.7183$. H_S in Eq. (1) is the $(2m_R + 1) \times (2m_T + 1)$ random scattering matrix with (ℓ, m)th element given by

$$\{H_S\}_{\ell,m} = \int_0^{\pi}\int_0^{\pi} g(\phi, \varphi)\mathrm{e}^{-i(\ell - m_R - 1)\varphi}\mathrm{e}^{i(m - m_T - 1)\phi} d\varphi d\phi,$$
$$\ell = 1, \cdots, 2m_R + 1, \quad m = 1, \cdots, 2m_T + 1. \tag{3}$$

Note that $\{H_S\}_{\ell,m}$ represents the complex gain of the scattering channel between the mth mode of the transmitter region and the ℓth mode of the receiver region, where $g(\phi, \varphi)$ is the scattering gain function, which is the effective random complex gain for signals leaving the transmitter aperture with angle of departure ϕ and arriving at the receiver aperture with angle of arrival φ.

[1] The 2D case is a special case of the 3D case where all the signals arrive from on a horizontal plane only. Similar results can be obtained using the 3D channel model proposed in [7].

[2] The set of modes form a basis of functions for representing a multipath wave field.

3. Exact PEP on correlated MIMO channels

Assume that perfect channel state information (CSI) is available at the receiver and also a maximum likelihood (ML) decoder is employed at the receiver. Assume that the codeword X was transmitted, but the ML-decoder chooses another codeword $\hat{X}$. Then the PEP, conditioned on the channel, is given by [1]

$$\mathrm{P}(X \to \hat{X}|h) = \mathrm{Q}\left(\sqrt{\frac{E_s}{2N_0} d^2(X,\hat{X})}\right), \tag{4}$$

where $d^2(X,\hat{X}) = h[I_{n_R} \otimes X_\Delta]h^\dagger$, $X_\Delta = (X-\hat{X})(X-\hat{X})^\dagger$, $h = (\mathrm{vec}\,(H^T))^T$ is a row vector. To compute the average PEP, we average Eq. (4) over the joint probability distribution of h. By using Craig's formula for the Gaussian Q-function [11, Chap. 4, Eq. (4.2)]

$$\mathrm{Q}(x) = \frac{1}{\pi}\int_0^{\pi/2} \exp\left(-\frac{x^2}{2\sin^2\theta}\right) d\theta$$

and the MGF-based technique presented in [4], we can write the average PEP as

$$\begin{aligned}\mathrm{P}(X \to \hat{X}) &= \frac{1}{\pi}\int_0^{\pi/2}\int_0^{\infty} \exp\left(-\frac{\Gamma}{2\sin^2\theta}\right) p_\Gamma(\Gamma) d\Gamma d\theta, \\ &= \frac{1}{\pi}\int_0^{\pi/2} \mathscr{M}_\Gamma\left(-\frac{1}{2\sin^2\theta}\right) d\theta, \end{aligned} \tag{5}$$

where $\mathscr{M}_\Gamma(s) = \int_0^\infty \mathrm{e}^{s\Gamma} p_\Gamma(\Gamma) d\Gamma$ is the MGF of

$$\Gamma = \frac{E_s}{2N_0} h[I_{n_R} \otimes X_\Delta]h^\dagger \tag{6}$$

and $p_\Gamma(\Gamma)$ is the probability density function (pdf) of Γ. Substituting Eq. (1) for H in $h = (\mathrm{vec}\,(H^T))^T$ and using the Kronecker product identity [12, p. 180] $\mathrm{vec}(AXB) = (B^T \otimes A)\,\mathrm{vec}\,(X)$, we rewrite Eq. (6) as

$$\Gamma = \frac{E_s}{2N_0} h_S (J_R^T \otimes J_T^\dagger)(I_{n_R} \otimes X_\Delta)(J_R^* \otimes J_T) h_S^\dagger \tag{7a}$$

$$= \frac{E_s}{2N_0} h_S \left[(J_R^\dagger J_R)^T \otimes (J_T^\dagger X_\Delta J_T)\right] h_S^\dagger \tag{7b}$$

$$= \frac{E_s}{2N_0} h_S G h_S^\dagger, \tag{7c}$$

where $h_S = (\mathrm{vec}(H_S{}^T))^T$ is a row vector and

$$G = (J_R^\dagger J_R)^T \otimes (J_T^\dagger X_\Delta J_T). \tag{8}$$

Note that, Eq. (7b) follows from Eq. (7a) via the identity [12, p. 180] $(A \otimes C)(B \otimes D) = AB \otimes CD$, provided that the matrix products AB and CD exist.

Note that $h_S G h_S^\dagger$ in Eq. (7c) is a quadratic form of a random variable since h_S is a random row vector and G is fixed as J_T, J_R and X_Δ are deterministic matrices. Furthermore, the matrix G is Hermitian as both $J_R^\dagger J_R$ and $J_T^\dagger X_\Delta J_T$ are Hermitian, and the Kronecker product between two Hermitian matrices is always Hermitian. The MGF associated with a quadratic random variable is readily found in the literature [3]. Using [3, Eq. (14)], we write the MGF of Γ as

$$\mathscr{M}_\Gamma(s) = \left[\det\left(I - \frac{s\bar{\gamma}}{2} RG\right)\right]^{-1}, \tag{9}$$

where $\bar{\gamma} = \frac{E_s}{N_0}$ is the average symbol energy-to-noise ratio (SNR) and $R = E\left\{h_S^\dagger h_S\right\}$ is the covariance matrix of h_S. Here we assumed that the entries of h_S are zero-mean complex Gaussian distributed.

Substitution of Eq. (9) into Eq. (5) gives the exact-PEP

$$\mathrm{P}(X \to \hat{X}) = \frac{1}{\pi}\int_0^{\pi/2} \left[\det\left(I + \frac{\bar{\gamma}}{4\sin^2\theta} RG\right)\right]^{-1} d\theta. \tag{10}$$

Remark 1: Equation (10) is the exact-PEP[3] of a space-time coded system applied to a spatially correlated slow fading MIMO channel following the channel decomposition in Eq. (1).

Remark 2: When $R = I$ (i.e., correlation between different communication modes is zero), Eq. (10) above captures the effects due to antenna spacing and antenna geometry on the performance of a space-time code operating over a slow fading channel.

Remark 3: When the fading channels are independent (i.e., $R = I$ and $G = I_{n_R} \otimes X_\Delta$), Eq. (10) simplifies to,

$$\mathrm{P}(X \to \hat{X}) = \frac{1}{\pi}\int_0^{\pi/2} \left[\det\left(I_{n_T} + \frac{\bar{\gamma}}{4\sin^2\theta} X_\Delta\right)\right]^{-n_R} d\theta,$$

which is the same as [4, Eq. (13)].

Kronecker product model as a special case. In some circumstances, the covariance matrix R of the scattering channel H_S can be expressed as a Kronecker product between correlation matrices observed at the receiver and the transmitter antenna arrays [13, 14], i.e.,

$$R = E\left\{h_S^\dagger h_S\right\} = F_R \otimes F_T, \tag{11}$$

where F_R and F_T are the transmit and receive correlation matrices. Substituting Eq. (11) in Eq. (10) and recalling the definition of G in Eq. (8), the exact-PEP can be written as

$$\mathrm{P}(X \to \hat{X}) = \frac{1}{\pi}\int_0^{\pi/2} \left[\det\left(I + \frac{\bar{\gamma}}{4\sin^2\theta} Z\right)\right]^{-1} d\theta\,, \tag{12}$$

where $Z = (F_R J_R^T J_R^*) \otimes (F_T J_T^\dagger X_\Delta J_T)$.

[3]Equation (10) can be evaluated in closed form using the analytical technique discussed in Section 4.

4. Realistic exact-PEP

The exact-PEP expression we derived in the previous section captures the antenna configurations (linear array, circular array, grid, etc.) both at the transmitter and the receiver arrays via J_T and J_R, respectively. Furthermore, it also incorporates the modal correlation effects at the transmitter and the receiver regions via F_T and F_R, respectively. Therefore, the PEP expression Eq. (12) can be considered as the *realistic* exact PEP of a space-time coded system.

To calculate the exact-PEP, one needs to evaluate the integral Eq. (12) (or Eq. (10) in a more general spatial scenario), either using numerical methods or analytical methods. We present an analytical technique which can be employed to evaluate the integral Eq. (12) in closed form as follows.

Matrix Z in Eq. (12) has size $M_R M_T \times M_R M_T$. Therefore, the integrand in Eq. (12) will take the form[4]

$$\left[\det\left(I+\frac{\bar{\gamma}}{4\sin^2\theta}Z\right)\right]^{-1}=\frac{(\sin^2\theta)^N}{\sum_{\ell=0}^{N}a_\ell(\sin^2\theta)^\ell}, \tag{13}$$

where $N=M_RM_T$ and a_ℓ, for $\ell=1,2,\cdots,N$, are constants. Note that the denominator of Eq. (13) is an Nth order polynomial in $\sin^2\theta$. To evaluate the integral Eq. (13) in closed form, we use the partial-fraction expansion technique given in [11, Appendix 5A] as follows.

First we begin by factoring the denominator of Eq. (13) into terms of the form $(\sin^2\theta+c_\ell)$, for $\ell=1,2,\cdots,N$. This involves finding the roots of an Nth order polynomial in $\sin^2\theta$ either numerically or analytically. Then Eq. (13) can be expressed in product form as

$$\frac{(\sin^2\theta)^N}{\sum_{\ell=0}^{N}a_\ell(\sin^2\theta)^\ell}=\prod_{\ell=1}^{\Lambda}\left(\frac{\sin^2\theta}{c_\ell+\sin^2\theta}\right)^{m_\ell}, \tag{14}$$

where m_ℓ is the multiplicity of the root c_ℓ and $\sum_{\ell=1}^{\Lambda}m_\ell=N$. Applying the partial-fraction decomposition theorem to the product form Eq. (14), we get

$$\prod_{\ell=1}^{\Lambda}\left(\frac{\sin^2\theta}{c_\ell+\sin^2\theta}\right)^{m_\ell}=\sum_{\ell=1}^{\Lambda}\sum_{k=1}^{m_\ell}A_{k\ell}\left(\frac{\sin^2\theta}{c_\ell+\sin^2\theta}\right)^{k}, \tag{15}$$

where the residual $A_{k\ell}$ is given by [11, Eq. (5A.72)]

$$A_{k\ell}=\frac{\left\{\frac{d^{m_\ell-k}}{dx^{m_\ell-k}}\prod_{\substack{n=1\\n\neq\ell}}^{\Lambda}\left(\frac{1}{1+c_nx}\right)^{m_n}\right\}|_{x=-c_\ell^{-1}}}{(m_\ell-k)!c_\ell^{m_\ell-k}}. \tag{16}$$

Expansion Eq. (15) often allows integration to be performed on each term separately by inspection. In fact, each term in Eq. (15) can be separately integrated using a result found in [4], where

$$\begin{aligned}P(c_\ell,k)&=\frac{1}{\pi}\int_0^{\pi/2}\left(\frac{\sin^2\theta}{c_\ell+\sin^2\theta}\right)^k d\theta,\\&=\frac{1}{2}\left[1-\sqrt{\frac{c_\ell}{1+c_\ell}}\sum_{j=0}^{k-1}\binom{2j}{j}\left(\frac{1}{4(1+c_\ell)}\right)^j\right].\end{aligned} \tag{17}$$

Now using the partial-fraction form of the integrand in Eq. (15) together with Eq. (17), we obtain the exact-PEP in closed form as

$$\begin{aligned}\mathrm{P}(X\to\hat{X})&=\frac{1}{\pi}\int_0^{\pi/2}\prod_{k=1}^{\Lambda}\left(\frac{\sin^2\theta}{c_\ell+\sin^2\theta}\right)^{m_\ell}d\theta,\\&=\sum_{\ell=1}^{\Lambda}\sum_{k=1}^{m_\ell}A_{k\ell}P(c_\ell,k).\end{aligned} \tag{18}$$

For the special case of distinct roots, i.e., $m_1=m_2=\cdots=m_N=1$, the exact-PEP is given by

$$\mathrm{P}(X\to\hat{X})=\frac{1}{2}\sum_{\ell=1}^{N}\left(1-\sqrt{\frac{c_\ell}{1+c_\ell}}\right)\prod_{\substack{n=1\\n\neq\ell}}^{N}\left(\frac{c_\ell}{c_\ell-c_n}\right).$$

5. Analytical performance evaluation: examples

In this section, we consider the following two space-time codes as examples:

- 4-state QPSK space-time trellis code with two transmit antennas [1, Fig. 4]; the shortest error event path of length 2, as illustrated by shading in Fig. 1 of [4];
- 16-state QPSK space-time trellis code with three transmit antennas [8, Table 1]; the shortest error event path of length 3.

For the 4-state code, the exact-PEP results and approximate bit error probability (BEP) results for $n_R=1$ and $n_R=2$ were presented in [2, 4] for i.i.d. fast fading and slow fading channels. In [5], the effects of fading correlation on the average BEP were studied for $n_R=1$ over a slow fading channel. In this work, we compare the i.i.d. channel performance results presented in [2, 4] with our realistic exact-PEP results for different antenna spacing and scattering distribution parameters. In addition, we use the 16-state code with three transmit antennas to study the impact of antenna placement on the performance of space-time codes.

In [2, 4], performances were evaluated under the assumption that the transmitted codeword is the all-zero codeword. Here we also adopt the same assumption as we compare our results with their results. However, we are aware that space-time codes may, in general, be nonlinear, i.e., the average BEP can depend on the transmitted codeword.

[4] One would need to evaluate the determinant of $\left(I+\frac{\bar{\gamma}}{4\sin^2\theta}Z\right)$ and then take the reciprocal of it to obtain the form Eq. (13).

5.1. Effect of antenna spacing

First we consider the effect of antenna spacing on the exact-PEP when the scattering environment is isotropic, i.e., $F_T = I_{2m_T+1}$ and $F_R = I_{2m_R+1}$. Consider the 4-state code with two transmit antennas and two receive antennas, where the two transmit antennas are placed in a circular aperture of radius 0.25λ (antenna separation[5] = 0.5λ) and the two receive antennas are placed in a circular aperture of radius r (antenna separation = $2r$).

Figure 1 shows the exact pairwise error probability performance of the 4-state code for length 2 error event and receive antenna separations 0.1λ, 0.2λ, 0.5λ and λ. Also shown in Fig. 1 for comparison is the exact-PEP for the i.i.d. slow fading channel (Rayleigh) corresponding to the length two error event path.

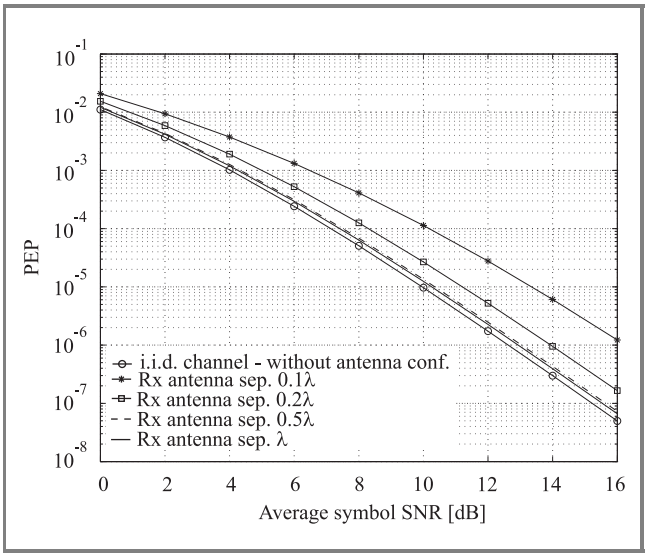

Fig. 1. Exact pairwise error probability performance of the 4-state space-time trellis code with 2-Tx antennas and 2-Rx antennas: length 2 error event.

As we can see from the figure, the effect of antenna separation on the exact-PEP is not significant when the receive antenna separation is 0.5λ or higher. However, the effect is significant when the receive antenna separation is small. For example, at PEP 10^{-5}, the realistic PEPs are 1 dB and 3 dB away from the i.i.d. channel performance results for 0.2λ and 0.1λ transmit antenna separations, respectively. From these observations, we can emphasize that the effect of antenna spacing on the performance of the 4-state code is minimum for higher antenna separations whereas the effect is significant for smaller antenna separations.

[5]In a 3D isotropic scattering environment, antenna separation 0.5λ (first null of the order zero spherical Bessel function) gives zero spatial correlation, but here we constraint our analysis to a 2D scattering environment. The spatial correlation function in a 2D isotropic scattering environment is given by a Bessel function of the first kind. Therefore, antenna separation $\lambda/2$ does not give zero spatial correlation in a 2D isotropic scattering environment.

5.2. Loss of diversity advantage due to a region with limited size

We now consider the diversity advantage of a space-time coded system as the number of receive antennas increases while the receive antenna array aperture radius remains fixed. Figure 2 shows the exact-PEP of the 4-state STTC

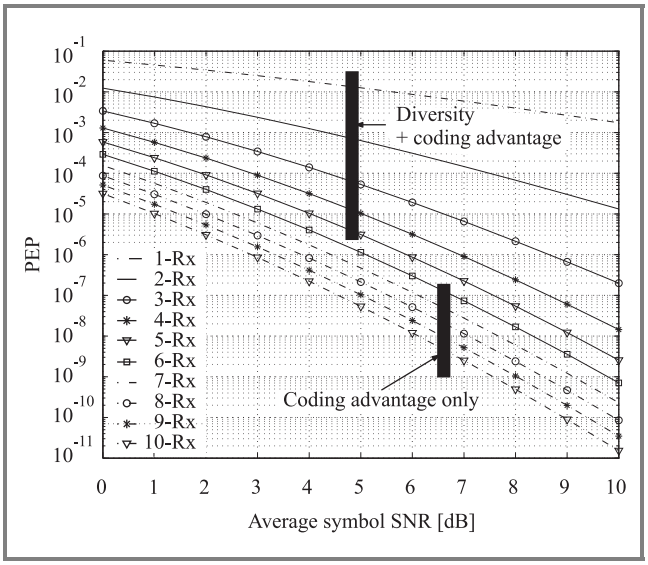

Fig. 2. Exact PEP performance of the 4-state space-time trellis code with 2-Tx antennas and n-Rx antennas: length 2 error event.

with two transmit antennas and n_R receive antennas, where $n_R = 1, 2, \ldots, 10$. The two transmit antennas are placed in a circular aperture of radius 0.25λ (antenna separation = 0.5λ) and n_R receive antennas are placed in a uniform circular array antenna configuration with radius 0.15λ. In this case, the distance between two adjacent receive antenna elements is $0.3\lambda \sin(\pi/n_R)$.

The slope of the performance curve on a log scale corresponds to the diversity advantage of the code and the horizontal shift in the performance curve corresponds to the coding advantage. According to the code construction criteria given in [1], the diversity advantage promised by the 4-state STTC is $2n_R$. With the above antenna configuration setup, however, we observed that the slope of each performance curve remains the same when $n_R > 5$, which results in zero diversity advantage improvement for $n_R > 5$. Nevertheless, for $n_R > 5$, we still observed some improvement in the coding gain, but the rate of improvement is slower with the increase in number of receive antennas. Here the loss of diversity gain is due to the fewer number of effective communication modes available at the receiver region than the number of antennas available for reception. In this case, from Eq. (2), the receive aperture of radius 0.15λ corresponds to $M = 2\lceil \pi e 0.15 \rceil + 1 = 5$ effective communication modes at the receive region. Therefore when $n_R > 5$, the diversity advantage of the code is determined by the number of effective communication modes available at the receiver

antenna region rather than the number of antennas available for reception. That is, the point where the diversity loss occurred is clearly related to the size of the antenna aperture, where smaller apertures result in diversity loss of the code for lower number of receive antennas, as proved analytically in [15].

5.3. Effect of antenna configuration

In this section, we compare the PEP performance of the 16-state code for different antenna configurations at the transmitter antenna array. Here we consider UCA and ULA antenna configurations as examples.[6] We place the three transmit antennas within a fixed circular aperture of radius $r(=0.15\lambda, 0.25\lambda)$, where the antenna placements are shown in Fig. 3. The exact-PEP performance for the error event path of length three is also shown in Fig. 3 for a single receive antenna.

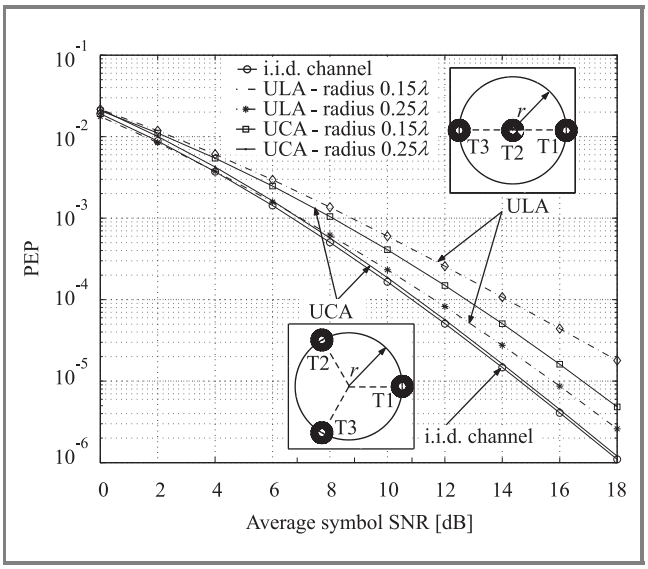

Fig. 3. The exact-PEP performance of the 16-state code with three transmit and one receive antennas for UCA and ULA transmit antenna configurations: length 3 error event.

From Fig. 3, it is observed that at high SNRs the performance given by the UCA antenna configuration outperforms that of the ULA antenna configuration. For example, at PEP 10^{-5}, the performance difference between UCA and ULA are 2.75 dB with 0.15λ receiver aperture radius and 1.25 dB with 0.25λ receiver aperture radius. From Fig. 3, we observed that as the radius of the transmitter aperture decreases the diversity advantage of the code is reduced, particularly for the ULA antenna configuration. Here, the loss of diversity advantage is mainly due to the loss of rank of J_T.

[6]The exact-PEP expression we derived in this work can be applied to any arbitrary antenna configuration.

5.4. Effect of modal correlation

For simplicity, here we only consider the modal correlation effects at the receiver region and assume that the effective communication modes available at the transmitter region are uncorrelated, i.e., $F_T = I_{2m_T+1}$. First, we derive the definition of modal correlation matrix F_R at the receiver region.

Using Eq. (3), we can define the modal correlation between complex scattering gains as

$$\gamma_{m,m'}^{\ell,\ell'} = E\left\{\{H_S\}_{\ell,m}\{H_S\}_{\ell',m'}^{*}\right\}.$$

Assume that the scattering from one direction is independent of that from another direction for both the receiver and the transmitter apertures. Then the second-order statistics of the scattering gain function $g(\phi,\varphi)$ can be defined as

$$E\left\{g(\phi,\varphi)g^{*}(\phi',\varphi')\right\} = G(\phi,\varphi)\delta(\phi-\phi')\delta(\varphi-\varphi'),$$

where $G(\phi,\varphi) = E\left\{|g(\phi,\varphi)|^2\right\}$ with normalization $\int\int G(\phi,\varphi)d\varphi d\phi = 1$. With the above assumption, the modal correlation coefficient, $\gamma_{m,m'}^{\ell,\ell'}$ can be simplified to

$$\gamma_{m,m'}^{\ell,\ell'} = \int\int G(\phi,\varphi)\mathrm{e}^{-i(\ell-\ell')\varphi}e^{i(m-m')\phi}d\varphi d\phi.$$

Then the correlation between the ℓth and ℓ'th modes at the receiver region due to the mth mode at the transmitter region is given by

$$\gamma_{\ell,\ell'}^{Rx} = \int \mathscr{P}_{Rx}(\varphi)\mathrm{e}^{-i(\ell-\ell')\varphi}d\varphi, \qquad (19)$$

where $\mathscr{P}_{Rx}(\varphi) = \int G(\phi,\varphi)d\phi$ is the normalized azimuth power distribution of the scatterers surrounding the receiver antenna region. Here we see that modal correlation at the receiver is independent of the mode selected from the transmitter region. Note that the (ℓ,ℓ')th element of F_R is given by Eq. (19) and F_R is a $(2m_R+1)\times(2m_R+1)$ matrix. Also note that $\mathscr{P}_{Rx}(\varphi)$ can be modeled using all common azimuth power distributions such as uniform, Gaussian, Laplacian, Von-Mises, polynomial, etc.

It was shown in [16] that all azimuth power distribution models give very similar correlation values for a given angular spread, especially for small antenna separations. Therefore, without loss of generality, we restrict our investigation only to the case of energy arriving uniformly over a limited angular spread σ around a mean AOA φ_0 (uniform limited azimuth power distribution). In this case, the modal correlation coefficient $\gamma_{\ell,\ell'}^{Rx}$ in the receiver region is given by

$$\gamma_{\ell,\ell'}^{Rx} = \mathrm{sinc}((\ell-\ell')\sigma)\mathrm{e}^{-i(\ell-\ell')\varphi_0}. \qquad (20)$$

Continuing the performance analysis, we now investigate the modal correlation effects on the performance of

the 4-state code with two transmit and two receive antennas. We place the two transmit antennas 0.5λ apart and also the two receive antennas 0.5λ apart.[7]

Figure 4 shows the exact-PEP performances of the 4-state code for various angular spreads $\sigma = \{5^\circ, 30^\circ, 45^\circ, 180^\circ\}$ about a mean AOA $\varphi_0 = 0^\circ$ from broadside, where the broadside angle is defined as the angle perpendicular to the line connecting the two antennas. Note that $\sigma = 180^\circ$ represents the isotropic scattering environment.

The exact-PEP performance for the i.i.d. slow fading channel (Rayleigh) is also plotted on the same graph for comparison.

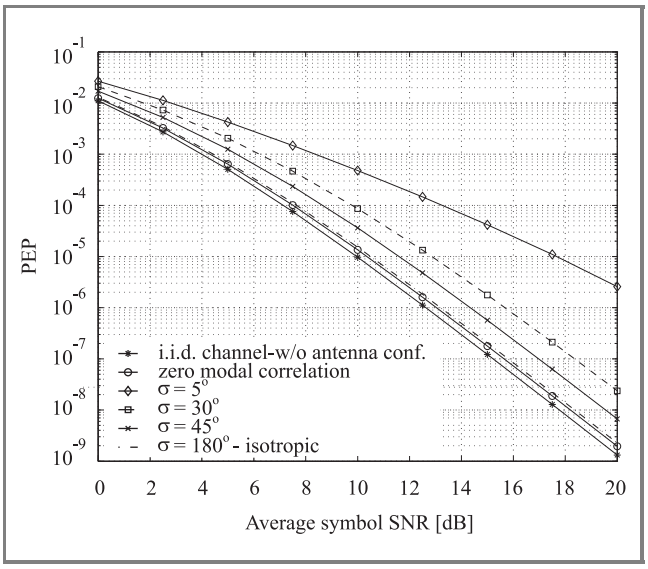

Fig. 4. Effect of receiver modal correlation on the exact-PEP of the 4-state QPSK space-time trellis code with 2-Tx antennas and 2-Rx antennas for the length 2 error event. Uniform limited power distribution with a mean angle of arrival $\varphi_0 = 0^\circ$ from broadside and angular spreads $\sigma = \{5^\circ, 30^\circ, 45^\circ, 180^\circ\}$.

As one would expect, the performance loss incurred due to the modal correlation increases as the angular spread of the distribution decreases.

For example, at PEP 10^{-5}, the realistic PEP results obtained from Eq. (12) are about 0.25 dB, 1.75 dB, 2.75 dB and 7.5 dB away from the i.i.d. channel performance results for angular spreads 180°, 45°, 30° and 5°, respectively. Therefore, in general, if the angular spread of the distribution is closer to 180° (isotropic scattering), then the loss incurred due to the modal correlation is insignificant, provided that the antenna spacing is optimal. However, for moderate angular spread values such as 45° and 30°, the performance loss is quite significant. This is due to the higher concentration of energy closer to the mean AOA for small angular spreads.

It is also observed that for large angular spread values, the diversity order of the code (the slope of the performance curve) is preserved whereas for small and moderate angular spread values, the diversity order of the code is diminished.

Figure 5 shows the PEP performance results of the 4-state code for a mean AOA $\varphi_0 = 60^\circ$ from broadside. Similar results are observed as for the mean AOA $\varphi_0 = 0^\circ$ case.

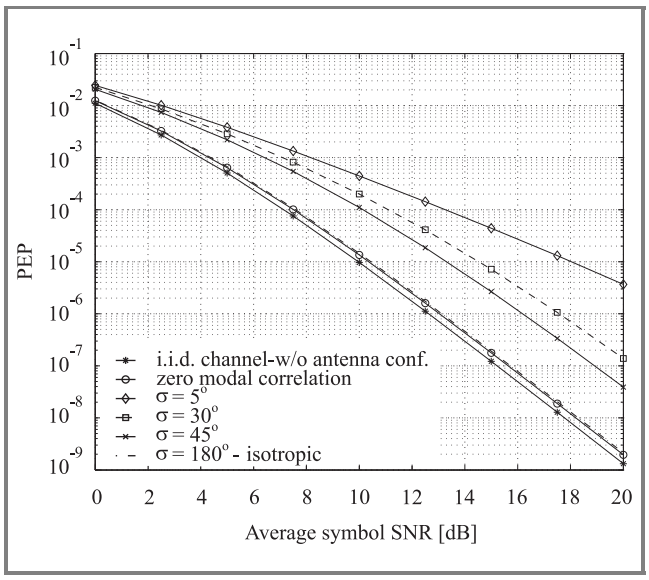

Fig. 5. Effect of receiver modal correlation on the exact-PEP of the 4-state QPSK space-time trellis code with 2-Tx antennas and 2-Rx antennas for the length 2 error event. Uniform limited power distribution with a mean angle of arrival $\varphi_0 = 60^\circ$ from broadside and angular spreads $\sigma = \{5^\circ, 30^\circ, 45^\circ, 180^\circ\}$.

Comparing Figs. 4 and 5 we observe that the performance loss is increased for all angular spreads as the mean AOA moves away from broadside. This can be justified by the reasoning that, as the mean AOA moves away from broadside, there will be a reduction in the angular spread exposed to the antennas and hence less signals being captured.

Furthermore, we observed that (performance results are not shown here) when there are more than two receive antennas in a fixed receiver aperture, the performance loss of the 4-state code with decreasing angular spread is most pronounced for the ULA antenna configuration when the mean AOA is closer to 90° (inline with the array). But, for the UCA antenna configuration, the performance loss is insignificant as the mean AOA moves away from broadside for all angular spreads. This suggests that the UCA antenna configuration is less sensitive to change of mean AOA compared to the ULA antenna configuration. Hence, the UCA antenna configuration is best suited to employ a space-time code.

Using the results we obtained thus far, we can claim that, in general, space-time trellis codes are susceptible to spatial fading correlation effects, in particular, when the antenna separation and the angular spread are small.

[7]Performance loss due to antenna spacing is minimum when the antenna separation is 0.5λ or higher as we showed in Subsection 5.1.

5.5. Extension of PEP to average bit error probability

An approximation to the average BEP was given in [17] on the basis of accounting for error event paths of lengths up to H as

$$P_b(E) \cong \frac{1}{b}\sum_t q(X \to \hat{X})_t P(X \to \hat{X})_t, \qquad (21)$$

where b is the number of input bits per transmission, $q(X \to \hat{X})_t$ is the number of bit errors associated with the error event t and $P(X \to \hat{X})_t$ is the corresponding PEP. In [4], it was shown that error event paths of lengths up to H are sufficient to achieve a reasonably good approximation to the full upper (union) bound that takes into account error event paths of all lengths. For example, with the 4-state STTC, error event paths of lengths up to $H = 4$ is sufficient for the slow fading channel.

The closed-form solution for average BEP of a space-time code can be obtained by finding closed-form solutions for PEPs associated with each error type, using the analytical technique given in Section 4. In previous sections, we investigate the effects of antenna spacing, antenna geometry and modal correlation on the exact-PEP of a space-time code over slow fading channel. The observations and claims which we made there, are also valid for the BEP case as the BEPs are calculated directly from PEPs. Therefore, to avoid repetition, we do not discuss BEP performance results here.

6. Conclusion

Using an MGF-based approach, we have derived an analytical expression for the exact pairwise error probability of a space-time coded system operating over a spatially correlated slow fading channel. This analytical PEP expression fully accounts for antenna separation, antenna geometry and surrounding azimuth power distributions, both at the receiver and the transmitter antenna arrays. In practice, it can be used as a tool to estimate or predict the performance of a space-time code under any antenna configuration and surrounding azimuth power distribution parameters. Based on this new PEP expression, we showed that space-time codes employed on multiple transmit and multiple receive antennas are susceptible to spatial fading correlation effects, particularly for small antenna separations and small angular spreads.

Acknowledgements

This work was supported by the Australian Research Council Discovery Grant DP0343804. Thushara D. Abhayapala is also with National ICT Australia, Locked Bag 8001, Canberra, ACT 2601, Australia. National ICT Australia is funded through the Australian Government's *Backing Australia's Ability* initiative, in part through the Australian Research Council.

References

[1] V. Tarokh, N. Seshadri, and A. R. Calderbank, "Space-time codes for high data rate wireless communication: performance criterion and code construction", *IEEE Trans. Inform. Theory*, vol. 44, no. 1, pp. 744–765, 1998.

[2] M. Uysal and C. N. Georghiades, "Error performance analysis of spacetime codes over Rayleigh fading channels", *J. Commun. Netw.*, vol. 2, no. 4, pp. 351–355, 2000.

[3] G. L. Turin, "The characteristic function of hermetian quadratic forms in complex normal random variables", *Biometrika*, vol. 47, no. 1–2, pp. 199–201, 1960.

[4] M. K. Simon, "Evaluation of average bit error probability for space-time coding based on a simpler exact evaluation of pairwise error probability", *Int. J. Commun. Netw.*, vol. 3, no. 3, pp. 257–264, 2001.

[5] M. Uysal and C. N. Georghiades, "Effect of spatial fading correlation on performance of space-time codes", *Electron. Lett.*, vol. 37, no. 3, pp. 181–183, 2001.

[6] T. D. Abhayapala, T. S. Pollock, and R. A. Kennedy, "Spatial decomposition of MIMO wireless channels", in *Proc. Seventh Int. Symp. Sig. Proces. Appl. ISSPA'2003*, Paris, France, 2003, vol. 1, pp. 309–312.

[7] T. D. Abhayapala, T. S. Pollock, and R. A. Kennedy, "Charakterization of 3D spatial wireless channels", in *IEEE Veh. Technol. Conf. (Fall) VTC 2003*, Orlando, USA, 2003.

[8] Z. Chen, B. Vucetic, J. Yuan, and K. L. Lo, "Space-time trellis codes with two, three and four transmit antennas in quasi-static flat fading channels", in *Proc. IEEE Int. Conf. Commun.*, New York, USA, 2002, pp. 1589–1595.

[9] L. Hanlen and M. Fu, "Wireless communications systems with spatial diversity: a volumetric approach", in *IEEE Int. Conf. Commun. ICC'2003*, Anchorage, USA, 2003, vol. 4, pp. 2673–2677.

[10] H. M. Jones, R. A. Kennedy, and T. D. Abhayapala, "On dimensionality of multipath fields: spatial extent and richness", in *Proc. IEEE Int. Conf. Acoust., Speech, Sig. Proces. ICASSP'2002*, Orlando, USA, 2002, vol. 3, pp. 2837–2840.

[11] M. K. Simon and M. S. Alouini, *Digital Communications over Fading Channels*, 2nd ed. Hoboken: Wiley, 2004.

[12] G. H. Golub and C. F. Van Loan, *Matrix Computations*, 3rd ed. Baltimore, London: The Johns Hopkins University Press, 1996.

[13] J. P. Kermoal, L. Schumacher, K. I. Pedersen, P. E. Mogensen, and F. Frederiksen, "A stochastic MIMO radio channel model with experimental validation", *IEEE J. Selec. Areas Commun.*, vol. 20, no. 6, pp. 1211–1226, 2002.

[14] T. S. Pollock, "Correlation modelling in MIMO systems: when can we Kronecker?", in *Proc. 5th Austr. Commun. Theory Worksh.*, Newcastle, Australia, 2004, pp. 149–153.

[15] T. A. Lamahewa, R. A. Kennedy, and T. D. Abhayapala, "Upper-bound for the pairwise error probability of space-time codes in physical channel scenarios", in *Proc. 5th Austr. Commun. Theory Worksh.*, Brisbane, Australia, 2005, pp. 26–32.

[16] T. S. Pollock, T. D. Abhayapala, and R. A. Kennedy, "Introducing space into MIMO capacity calculations", *J. Telecommun. Syst.*, vol. 24, no. 2, pp. 415–436, 2003.

[17] J. K. Cavers and P. Ho, "Analysis of the error performance of trellis coded modulations in Rayleigh fading channels", *IEEE Trans. Commun.*, vol. 40, no. 1, pp. 74–83, 1992.

Tharaka A. Lamahewa received the B.E. (hons.) degree in information technology and telecommunications engineering from the University of Adelaide, South Australia, in 2000. He is currently pursuing the Ph.D. degree in telecommunications engineering at the Research School of Information Sciences and Engineering, Australian National University, Canberra. From 2001 to 2003, he worked as a software engineer at Motorola Electronics Pvt Ltd., Singapore. His research interests include space-time coding, MIMO channel modeling and MIMO capacity analysis for wireless communication systems.

e-mail: tharaka.lamahewa@anu.edu.au
Department of Information Engineering
Research School of Information Sciences and Engineering
The Australian National University
Canberra, ACT 0200, Australia

Marvin K. Simon is currently a Principal Scientist at the Jet Propulsion Laboratory, California Institute of Technology, Pasadena, USA, where for the last 36 years he has performed research as applied to the design of NASA's deep-space and near-earth missions resulting in the issuance of 9 patents, 25 NASA Tech Briefs and 4 NASA Space Act awards. Doctor Simon is known as an internationally acclaimed authority on the subject of digital communications with particular emphasis in the disciplines of modulation and demodulation, synchronization techniques for space, satellite and radio communications, trellis-coded modulation, spread spectrum and multiple access communications, and communication over fading channels. He has published over 200 papers on the above subjects and is co-author of 11 textbooks. He is the co-recipient of the 1988 Prize Paper Award in Communications of the "IEEE Transactions on Vehicular Technology" for his work on trellis coded differential detection systems and also the 1999 Prize Paper of the IEEE Vehicular Technology Conference for his work on switched diversity. He is a Fellow of the IEEE and a Fellow of the IAE. Among his awards are the NASA Exceptional Service Medal, NASA Exceptional Engineering Achievement Medal, IEEE Edwin H. Armstrong Achievement Award and the IEEE Millennium Medal all in recognition of outstanding contributions to the field of digital communications and leadership in advancing this discipline.

e-mail: marvin.k.simon@jpl.nasa.gov
Jet Propulsion Laboratory
California Institute of Technology
Pasadena, CA 91109, USA

Thushara D. Abhayapala was born in Colombo, Sri Lanka, in 1967. He received the B.E. degree in interdisciplinary systems engineering in 1994 and the Ph.D. degree in telecommunications engineering in 1999 from the Australian National University (ANU). From 1995 to 1997, he worked as a research engineer at the Arthur C. Clarke Centre for Modern Technologies, Sri Lanka. Since December 1999, Associate Professor Abhayapala has been with the Department of Information Engineering, Research School of Information Sciences and Engineering at the ANU. Currently he is a principal researcher and the program leader for Wireless Signal Processing program, National ICT Australia (NICTA), Canberra. His research interests are in the areas of space-time signal processing for wireless communication systems, spatio-temporal channel modeling, MIMO capacity analysis, UWB systems, array signal processing and acoustic signal processing. He has supervised 17 research students and co-authored approximately 100 papers. Doctor Abhayapala is currently an associate editor for EURASIP Journal on Wireless Communications and Networking.

e-mail: thushara.abhayapala@anu.edu.au.
Department of Information Engineering
Research School of Information Sciences and Engineering
The Australian National University
Canberra, ACT 0200, Australia

Rodney A. Kennedy has degrees from the University of New South Wales, Australia, University of Newcastle, and the Australian National University. He worked 3 years for CSIRO on the Australia Telescope Project. He is now with the Department of Information Engineering, Research School of Information Sciences and Engineering at the Australian National University. His research interests are in the fields of digital and wireless communications, digital signal processing and acoustical signal processing.

e-mail: rodney.kennedy@anu.edu.au
Department of Information Engineering
Research School of Information Sciences and Engineering
The Australian National University
Canberra, ACT 0200, Australia